COMMUNICATION

Conformable Solid-Index Phase Masks Composed of High-Aspect-Ratio Micropillar Arrays and Their Application to 3D Nanopatterning

*Junyong Park, Jae Hong Park, Eunhye Kim, Chi Won Ahn, Hyun Ik Jang, John A. Rogers, and Seokwoo Jeon**

Three-dimensional (3D) microstructures are essential elements in various technological applications, including optical coatings,[1,2] tissue engineering scaffolds,[3] microfluidics,[4] energy storage devices,[5,6] plasmonics,[7] and photonic crystals.[8,9] While conventional methods, such as photolithography and electron beam lithography, are costly and ineffective in the generation of complex 3D patterns over large areas, unconventional methods based on soft lithography, such as nanoimprint lithography (NIL),[10] nanotransfer printing (nTP),[11] microcontact printing (μCP),[12] and micromolding in capillaries (MIMIC),[13] provide simple and inexpensive routes to fabricate complex multidimensional nanostructures. Above all, proximity field nanopatterning (PnP),[14] which uses elastomeric components similar to those used in soft lithography, can generate complex 3D nanostructures very rapidly over large areas. Optical interference from the conformable elastomers, working as phase shift elements, generates a complex 3D intensity distribution by the Talbot effect,[15] or self-imaging effect. The diffracted images of surface relief structures are periodically repeated at integer or fractional Talbot distances from the surface of the mask.

Pattern resolution in soft lithography is mainly determined by the fineness and the aspect ratio of elastomeric surface relief structures, which generally consist of poly(dimethylsiloxane) (PDMS), from a Si master that contains the desired relief patterns on its surface. The height of the relief structures is particularly important in PnP because it defines the magnitude of the phase shift as a function of the refractive index and the wavelength of the incident light.[16] Hence, relief structures with a high aspect ratio and narrow spacings (<1 μm) between features must be well-controlled (i.e., straightness, duty cycle). Currently, two critical issues complicate control of these requirements. The first issue is the limited thickness and physical damage of a patterned photoresist on a Si wafer that serves as a master; a thicker resist can lead to greater difficulty and a higher potential for damage during the photopatterning and replication processes. The second issue is the low Young's modulus of soft elastomers (≈2–9 MPa),[17] which causes a collapse or a break in the neck of elastomeric relief structures, even after fine replication from the master. The low mechanical property also results in problems such as surface wrinkling,[18] sagging, buckling, and deforming[19,20] of the elastomers. Thus, reproducibility of the patterning cannot be guaranteed when using conformal contact-dependent methods. Several mold materials, such as polyolefin,[21] modified polyurethane,[22] PDMS,[23,24] and perfluoropolyether (PFPE),[25] have been proposed to increase the Young's modulus and aspect ratio of the relief structures. Nevertheless, dense and fine relief structures with a high aspect ratio composed of modified elastomers are still collapsed in the sub-micrometer range, and new rigid materials lose their conformability or wettability due to the high modulus when coming into contact with a resist-coated substrate.

In this study, we overcome the thickness and damage issues associated with photoresists by fabricating deep etched Si masters with relief structures made of Si itself. The collapse problem of high relief structures is solved by using high-modulus polyurethane acrylate (PUA). The PUA replica peels away directly from the masters with various back-supporting substrates. Using these back-supported PUA micropillars as binary phase shift elements, highly ordered 3D nanostructures can be fabricated by PnP in a single exposure step. A new design of a phase mask, which consists of a thin PDMS layer[26] on the PUA mask as a sticking layer, is proposed to improve the conformal contact between the high-modulus PUA mask and photoresist films, which is only possible because the high-aspect-ratio pillars satisfy the optimized amount of phase shift. This solid-index mask keeps relief structures from any type of undesired deformation (i.e., sagging, bending) during conformal contact because the PDMS layer holds the high relief structures in position compared to conventional air-gap phase mask. A thin film (≈10 μm) of 3D nanostructures patterned from the conformable solid-index phase mask shows high uniformity over

J. Park, E. Kim, Prof. S. Jeon
Department of Materials Science and Engineering
KAIST Institute for Nanocentury
Korea Advanced Institute of Science and Technology (KAIST)
Daejeon, 305 – 701, Republic of Korea
E-mail: jeon39@kaist.ac.kr
Dr. J. H. Park, Dr. C. W. Ahn, H. I. Jang,
Nano Fusion Technology Division
National Nanofab Center
Korea Advanced Institute of Science and Technology (KAIST)
Daejeon, 305 – 701, Republic of Korea
Prof. J. A. Rogers
Departments of Materials Science and Engineering
Chemistry, Mechanical Science and Engineering
Electrical and Computer Engineering
Beckman Institute for Advanced Science and Technology,
and Frederick Seitz Materials Research Laboratory
University of Illinois at Urbana-Champaign
Urbana, Illinois 61801, USA

DOI: 10.1002/adma.201003885

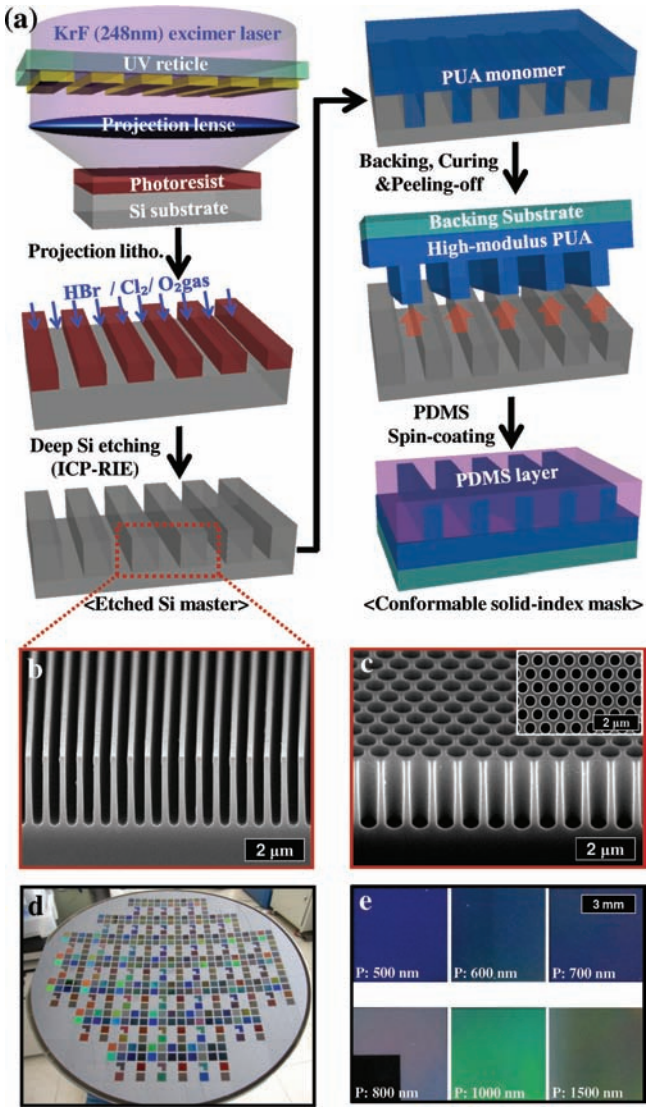

Figure 1. a) Schematic diagram illustrating the fabrication of conformable solid-index phase mask. b) Cross-sectional SEM image of line arrays of deep trenches with a relief depth of ≈2.5 μm. c) Cross-sectional and top SEM images of hexagonal arrays of microholes with a relief depth of ≈2.5 μm. d) Optical image of uniformly etched Si masters on an 8-in. wafer. e) Diffraction colors of different periodicities ranging from 500 nm to 1500 nm at the same relief depth.

a large area and superior absorption or reflection properties in the broadband light as a 3D light scattering medium, implying that it may be useful for broadband optical filters and partially dielectric absorbers for high-power ultrafast laser[27] or solar cell devices[28,29] via an inexpensive and simple route.

A schematic illustration of the overall experiment, including the deep Si etching and molding processes, is shown in **Figure 1**a. A detailed description is given in the Supporting Information. The Si masters used to replicate the micropillar arrays with relief depths that range from 100 nm to 2.5 μm were prepared by inductively coupled plasma reactive ion etching (ICP-RIE). While the cleaning and durability of conventional masters that consist of photoresist are limited due to the potential for mechanical, chemical, or thermal damages to the patterned photoresist, the etched Si masters sustain no damage, even after numerous replications. Even when some residue (i.e., a clogged hole, uncured monomer) remains after the replication process, thermal or chemical removal of the residue does not degrade the master. Figure 1b,c show a scanning electron microscopy (SEM) image of line arrays of deep etched Si trenches with a line width of 300 nm and a relief depth (h) of ≈2.5 μm and hexagonal arrays of holes with a diameter (d) of 520 nm, a periodicity (p) of 700 nm, and h of ≈2.5 μm. These 2D periodic sub-microstructures are uniformly formed on an 8-in. Si wafer that includes 37 repeated units of the desired master; this was designed to include line, square, and hexagonal arrays of microholes with various diameters, spacings, and periodicities (Figure 1d). Although the masters have the same relief depth and share similar geometry, the diffraction colors of each pattern are diversified by changes in the periodicity (Figure 1e).

First, using the etched Si masters, which consist of hexagonal arrays of microholes with d = 380 nm to 1 μm, p = 500 nm to 1.5 μm, spacings (w) = 120 nm to 500 nm and h = 1 μm (**Figure 2**a), the replication processes of an elastomer with high-modulus PDMS (h-PDMS) and PUA was conducted. The lateral collapse of the pillars becomes significant in the case of h-PDMS as the aspect ratio increases (Figure 2b). It has been demonstrated that high-aspect-ratio micropillar arrays can collapse under their own weight (ground collapse) or by adhesion to each other (lateral collapse) when adhesive force or capillary force is sufficiently large to cause contact between them.[24] Using the lateral collapse theory established by Hui et al.,[30] the critical elastic modulus of a lateral collapse for micropillar array is given by Equation 1,[17]

$$E_c^* = \frac{5/32 \times h^3 \gamma_s (1-\nu^2)^{1/4}}{d^{5/2}\omega^{3/2}} \quad (1)$$

where ν is the Poisson ratio and is the surface tension. If the Young's modulus of the replicating material is greater than E_c^*, there is no lateral collapse. The critical elastic modulus of each pattern for the PDMS and PUA were calculated (Supporting Information, Table S1). Compared to the maximized elastic modulus of PDMS at only ≈9 MPa,[24] the cured PUA used here has a high rigidity (≈1.7 GPa), which is sufficiently greater than E_c^*. As calculated, Figure 2c shows the successful replication of PUA micropillars with a high aspect ratio and a narrow spacing. Although replication of PDMS pillars from a Si master with a high aspect ratio in the sub-micrometer scale is limited due to the low Young's modulus of PDMS, replication of PDMS hole arrays from a PUA master with high-aspect-ratio pillars is wholly successful (Figure 2d). These high-aspect-ratio hole arrays can be very useful in the extension of patterning capabilities to various fields, including soft lithography and plasmonics.[7]

Backing layers are required for easy handling in the use of PUA micropillar arrays for various applications. **Figure 3**a shows an SEM image of tightly back-supported high-aspect-ratio (>6) micropillar arrays whose h is ≈2.5 μm and w is ≈120 nm. Various backing materials such as different types of glass, soft PDMS (Sylgard184), a ultrathin PUA film (10 μm), and a flexible polycarbonate film can be used as an imprinting mold, a

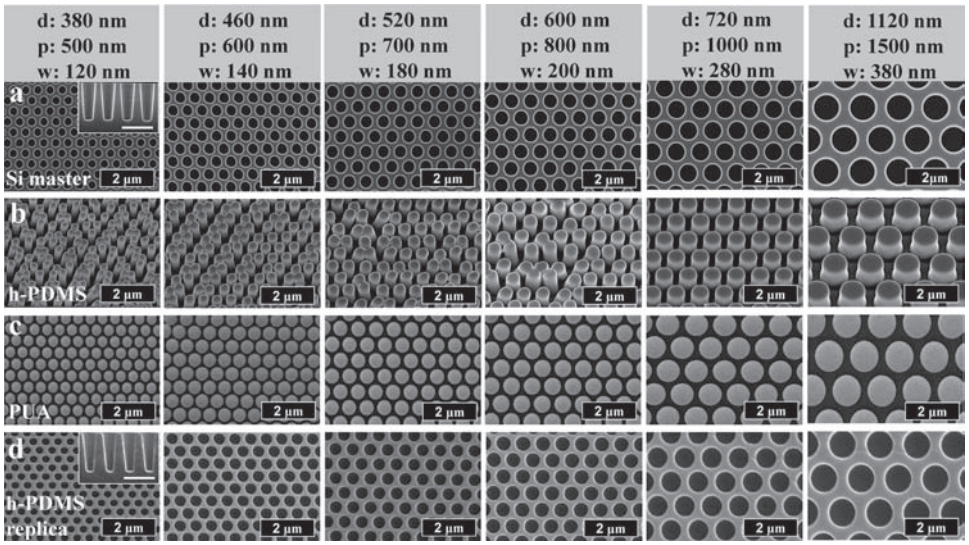

Figure 2. SEM images of a) etched Si masters with diameters of 380 nm to 1120 nm, periodicities of 500 nm to 1500 nm, and spacings of 120 nm to 380 nm (inset: cross-sectional view; scale bar 1 μm). b) h-PDMS micropillars replicated from Si masters. c) PUA micropillars replicated from Si masters. d) h-PDMS hole structures replicated from PUA masters of (c) (inset: cross-sectional view; scale bar 1 μm).

phase mask, or an optical coating (Supporting Information, Figure S1). These back-supported microstructures are easily peeled off from Si masters without surface treatment due to the low surface energy (≈25 dyne cm^{-1}) of the PUA used here.[22] Using these back-supported micropillar arrays, we examined the optical properties of PUA films and applied them to PnP as binary phase shift masks to fabricate high-quality complex 3D nanostructures. The PUA film shows good optical properties, such as high transmission and a high refractive index (≈1.54) compared to PDMS (≈1.4) (Figure 3b). The higher refractive index is advantageous for PnP because it increases the diffraction efficiency and minimizes the zero-order transmission.[31,32]

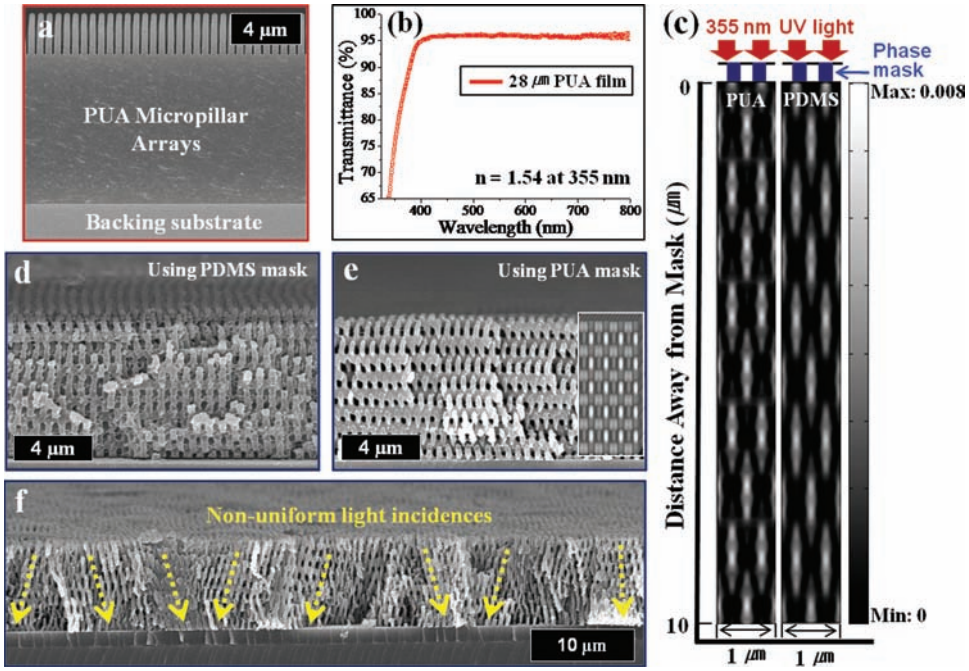

Figure 3. a) Cross-sectional SEM image of back-supported PUA micropillars with a high relief depth (≈2.5 μm) and a narrow spacing (≈120 nm). b) Transmittance spectrum of a thin PUA film (≈28 μm). c) Comparison of the 2D intensity distribution using PUA and PDMS phase masks with a relief depth of 420 nm (≈π phase shift condition) simulated by finite element modeling. d) Cross-sectional SEM image of 3D nanostructures using a PDMS mask with a relief depth of 420 nm and a periodicity of 500 nm. e) Cross-sectional SEM image of 3D nanostructures with high-resolution macropores (≈100 nm) using a PUA mask (inset: 3D simulation result conducted by rigorous coupled wave analysis (RCWA)). f) Cross-sectional SEM image of non-uniform 3D nanostructures due to the low conformability.

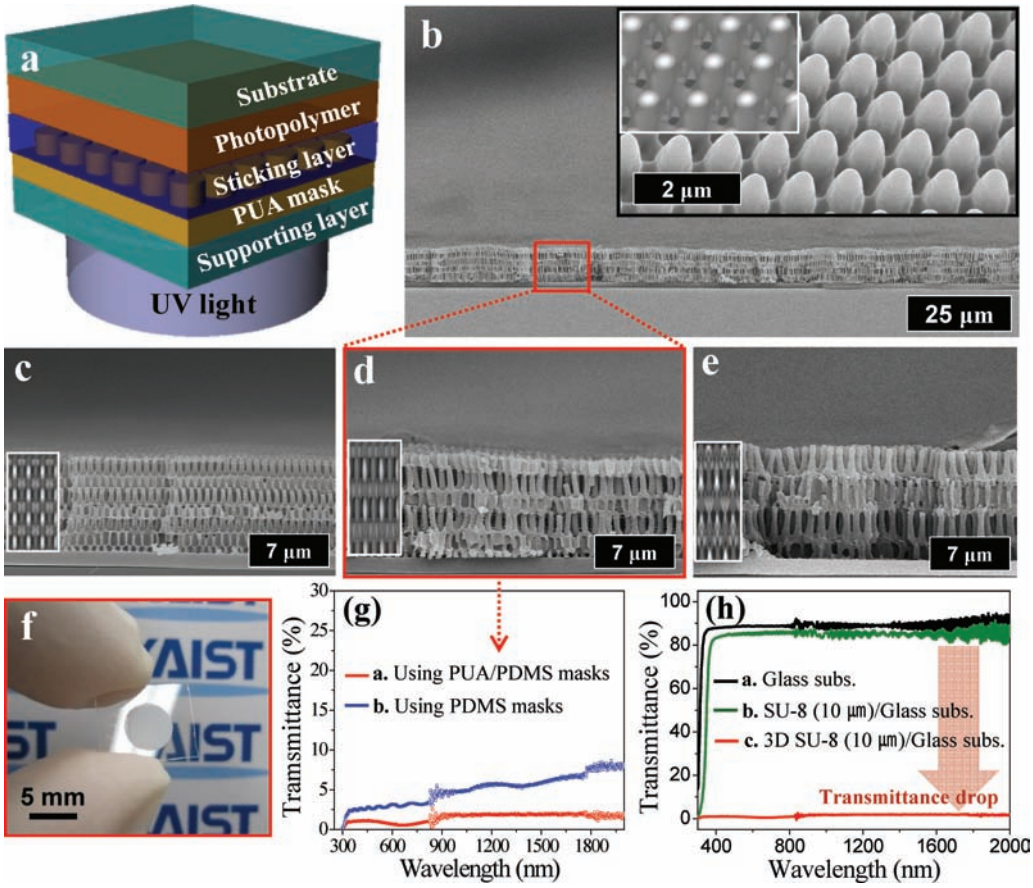

Figure 4. a) Schematic illustration of PnP using a PUA/PDMS solid-index phase mask. b) Cross-sectional SEM images of 3D nanostructures with high uniformity over large areas (inset: tilted-top view with a 3D simulation result conducted by RCWA). c–e) Highly ordered 3D nanostructures with different pore sizes due to different periodicities (600 nm, 800 nm, and 1 μm) of binary phase masks (inset: 3D simulation result by RCWA). f) Optical image of a visible opaque coating using 3D nanostructures. g) Transmittance spectra of 3D nanostructures patterned using PDMS and composite phase masks. h) Transmittance spectra of a glass substrate, a resist-coated glass substrate, and a 3D nanostructured resist-coated substrate.

As the result, better 3D intensity contrast can be generated in photoresists as UV light passes through a PUA compared to a PDMS mask (Figure 3c). Moreover, the rigid PUA compensates several contact problems of soft elastomers, such as sagging or deforming of micropillars when it comes into contact with a resist-coated substrate. These advantages make it possible to fabricate 3D nanostructures with ≈100 nm pores at a higher resolution much more easily through a PUA mask than through a conventional PDMS mask (Figure 3d,e). However, the PUA has relatively poor conformal contact between the mask and the photosensitive material due to its high Young's modulus. This leads to the occurrence of locally non-uniform structures in large-area patterning due to the slight changes in the direction of the normal incident light at the surface of the photoresist film (Figure 3f).

To overcome the low conformability or wettability of rigid PUA, we employed a PUA/PDMS composite phase mask, which consisted of thin PDMS (≈7 μm) films on PUA micropillar arrays as the sticking layers. The conformable solid-index mask also helps to reduce undesired deformation of relief structures so that patterned 3D nanostructures have better uniformity. The deformation changes distances between relief structures and degrades the straightness of side wall, which finally degrades 3D patterning resolution by modifying the light path during exposure. With this solid-index phase mask, the phase shift condition is slightly changed. In general, the π phase shift condition is well-known for its ability to generate the highest intensity contrast. The phase difference $\varphi(x)$ is given by Equation 2,[16]

$$\varphi(x) = \frac{2\pi}{\lambda}\Delta n u(x) \quad (2)$$

where Δn is the difference between refractive index of the material and the surrounding, $u(x)$ is the relief depth of the mask, and λ is the incident wavelength. From this equation, high relief structures above 1 μm must be generated near the π phase shift condition for PUA/PDMS composite phase masks, as the Δn (≈0.14) of the composite mask between the PUA and PDMS is much lower than the Δn (≈0.4) of a PDMS mask between PDMS and air. The deep etched Si master in this work makes it possible to generate high-aspect-ratio masks. **Figure 4**a shows a schematic illustration of PnP using a conformable solid-index phase mask with a PUA micropillar height of 1 μm, and Figure 4b shows highly ordered 3D nanostructures

with high uniformity over large areas patterned from this composite mask. The shape and the porosity of 3D nanostructures are easily diversified by changing a periodicity of micropillar arrays (Figure 4c–e). All of these experimental results are consistent with theoretical simulations using rigorous coupled wave analysis (RCWA) (insets in Figure 4b–e). The resist-coated glass with the improved 3D nanostructures appears opaque (Figure 4f) and transmits <1% of visible light and <2% of near-IR, which is evidence of better light scattering properties compared to 3D nanostructures patterned from PDMS masks (Figure 4g). This unique optical property is not from the photoresist film (≈10 μm) but from the light scattering of the 3D nanostructures (Figure 4h). Thus far, 2D periodic structures have been thoroughly researched and have consequently been used as light-trapping structures or absorbers, whereas their counterpart 3D structures have not been actively used. The absorption properties of 3D nanostructures are much better than these properties of 2D periodic structures, due to the increased length of the optical path through diffraction and trapping higher order diffraction.[33]

In summary, Si masters with a high relief depth are prepared by deep Si etching techniques, and defect-free micropillar arrays with a high aspect ratio (>6) and a narrow spacing (≈120 nm) are replicated from the masters with various backing substrates. Using back-supported micropillar arrays as binary phase masks, high-resolution 3D nanostructures are fabricated through PnP. The low conformability problem associated with the high-modulus PUA is solved by employing a new composite phase mask. The thin film (≈10 μm) of 3D nanostructures with high uniformity over a large area using the conformable solid-index mask offers superb optical properties. These new designs of phase masks and the outcome reported here can extend 3D patterning capabilities and improve the quality of 3D nanostructures for device applications.

Supporting Information

Supporting Information is available from the Wiley Online Library or from the author.

Acknowledgements

This work was supported by the grant from Center for Nanoscale Mechatronics & Manufacturing, one of the 21st Century Frontier Research Programs, which are supported by Ministry of Education, Science and Technology, KOREA, and the Low Observable Technology Research Center program of the Defense Acquisition Program Administration and Agency for Defense Development.

Received: October 21, 2010
Revised: November 19, 2010
Published online: January 10, 2011

[1] H. Y. Koo, D. K. Yi, S. J. Yoo, D. Y. Kim, *Adv. Mater.* **2004**, *16*, 274.
[2] H. Hattori, *Adv. Mater.* **2001**, *13*, 51.
[3] R. A. Barry, R. F. Shepherd, J. N. Hanson, R. G. Nuzzo, P. Wiltzius, J. A. Lewis, *Adv. Mater.* **2009**, *21*, 2407.
[4] S. Jeon, V. Malyarchuk, J. O. White, J. A. Rogers, *Nano Lett.* **2005**, *5*, 1351.
[5] J. W. Long, B. Dunn, D. R. Rolison, H. S. White, *Chem. Rev.* **2004**, *104*, 4463.
[6] T. Brezesinski, J. Wang, S. H. Tolbert, B. Dunn, *Nat. Mater.* **2010**, *9*, 146.
[7] J. M. Yao, A. P. Le, S. K. Gray, J. S. Moore, J. A. Rogers, R. G. Nuzzo, *Adv. Mater.* **2010**, *22*, 1102.
[8] Y. A. Vlasov, X. Z. Bo, J. C. Sturm, D. J. Norris, *Nature* **2001**, *414*, 289.
[9] G. M. Gratson, F. Garcia-Santamaria, V. Lousse, M. J. Xu, S. H. Fan, J. A. Lewis, P. V. Braun, *Adv. Mater.* **2006**, *18*, 461.
[10] L. J. Guo, *Adv. Mater.* **2007**, *19*, 495.
[11] J. Zaumseil, M. A. Meitl, J. W. P. Hsu, B. R. Acharya, K. W. Baldwin, Y. L. Loo, J. A. Rogers, *Nano Lett.* **2003**, *3*, 1223.
[12] J. L. Wilbur, A. Kumar, E. Kim, G. M. Whitesides, *Adv. Mater.* **1994**, *6*, 600.
[13] E. Kim, Y. N. Xia, G. M. Whitesides, *Adv. Mater.* **1996**, *8*, 245.
[14] S. Jeon, J. U. Park, R. Cirelli, S. Yang, C. E. Heitzman, P. V. Braun, P. J. A. Kenis, J. A. Rogers, *Proc. Natl. Acad. Sci. USA* **2004**, *101*, 12428.
[15] P. Latimer, R. F. Crouse, *Appl. Opt.* **1992**, *31*, 80.
[16] J. A. Rogers, K. E. Paul, R. J. Jackman, G. M. Whitesides, *J. Vac. Sci. Technol. B* **1998**, *16*, 59.
[17] Y. Zhang, C. W. Lo, J. A. Taylor, S. Yang, *Langmuir* **2006**, *22*, 8595.
[18] S. Yang, K. Khare, P. C. Lin, *Adv. Funct. Mater.* **2010**, *20*, 2550.
[19] K. J. Hsia, Y. Huang, E. Menard, J. U. Park, W. Zhou, J. Rogers, J. M. Fulton, *Appl. Phys. Lett.* **2005**, *86*, 154106.
[20] T. W. Odom, J. C. Love, D. B. Wolfe, K. E. Paul, G. M. Whitesides, *Langmuir* **2002**, *18*, 5314.
[21] G. Csucs, T. Kunzler, K. Feldman, F. Robin, N. D. Spencer, *Langmuir* **2003**, *19*, 6104.
[22] S. J. Choi, P. J. Yoo, S. J. Baek, T. W. Kim, H. H. Lee, *J. Am. Chem. Soc.* **2004**, *126*, 7744.
[23] F. Hua, Y. G. Sun, A. Gaur, M. A. Meitl, L. Bilhaut, L. Rotkina, J. F. Wang, P. Geil, M. Shim, J. A. Rogers, A. Shim, *Nano Lett.* **2004**, *4*, 2467.
[24] H. Schmid, B. Michel, *Macromolecules* **2000**, *33*, 3042.
[25] T. T. Truong, R. S. Lin, S. Jeon, H. H. Lee, J. Maria, A. Gaur, F. Hua, I. Meinel, J. A. Rogers, *Langmuir* **2007**, *23*, 2898.
[26] D. J. Shir, E. C. Nelson, D. Chanda, A. Brzezinski, P. V. Braun, J. A. Rogers, P. Wiltzius, *J. Vac. Sci. Technol. B* **2010**, *28*, 783.
[27] T. R. Schibli, K. Minoshima, H. Kataura, E. Itoga, N. Minami, S. Kazaoui, K. Miyashita, M. Tokumoto, Y. Sakakibara, *Opt. Express* **2005**, *13*, 8025.
[28] M. Agrawal, P. Peumans, *Opt. Express* **2008**, *16*, 5385.
[29] J. R. Nagel, M. A. Scarpulla, *Opt. Express* **2010**, *18*, A139.
[30] C. Y. Hui, A. Jagota, Y. Y. Lin, E. J. Kramer, *Langmuir* **2002**, *18*, 1394.
[31] Y. Bourgin, Y. Jourlin, O. Parriaux, A. Talneau, S. Tonchev, C. Veillas, P. Karvinen, N. Passilly, A. R. M. Zain, R. M. De La Rue, J. Van Erps, D. Troadec, *Opt. Express* **2010**, *18*, 10557.
[32] S. Jeon, D. J. Shir, Y. S. Nam, R. Nidetz, M. Highland, D. G. Cahill, J. A. Rogers, M. F. Su, I. F. El-Kady, C. G. Christodoulou, G. R. Bogart, *Opt. Express* **2007**, *15*, 6358.
[33] D. Shir, J. Yoon, D. Chanda, J.-H. Ryu, J. A. Rogers, *Nano Lett.* **2010**, *10*, 3041.